



Itaconate attenuates autoimmune hepatitis via PI3K/AKT/mTOR pathway-mediated inhibition of dendritic cell maturation and autophagy

Qiyu Zhang^{a,b,d}, Yang Luo^{c,e}, Qiuxia Zheng^a, Haixia Zhao^a, Xiaofeng Wei^{a,c},
Xun Li^{a,b,c,d,e,*}

^a The First School of Clinical Medicine, Lanzhou University, 730000 Lanzhou, China

^b Department of General Surgery, The First Hospital of Lanzhou University, 730000 Lanzhou, China

^c Key Laboratory of Biotherapy and Regenerative Medicine of Gansu Province, The First Hospital of Lanzhou University, 730000 Lanzhou, China

^d Hepatopancreatobiliary Surgery Institute of Gansu Province, The First Hospital of Lanzhou University, 730000 Lanzhou, China

^e Medical Frontier Innovation Research Center, The First Hospital of Lanzhou University, 730000 Lanzhou, China

ARTICLE INFO

Keywords:

Autoimmune hepatitis
Itaconate
Dendritic cell
Autophagy
PI3K/AKT/mTOR

ABSTRACT

Autoimmune hepatitis (AIH) results from an autoimmune-mediated chronic inflammatory response against liver cells. Defective self-tolerance and dysfunctional dendritic cells (DCs) play a regulatory role in AIH. Itaconate has recently attracted attention in the field of immunometabolism because of its crucial role as an anti-inflammatory metabolite that negatively regulates the inflammatory response. However, the underlying mechanism of itaconate mediation of DCs in AIH remains unclear. In this study, we found that itaconate acts as an anti-inflammatory factor in the liver. Endogenous itaconate levels were significantly increased in mice with S100-induced AIH model and correlated with upregulation of the immune-responsive gene 1 expression. However, the anti-inflammatory response from endogenously itaconate may not represent the effects exogenously-produced itaconate. We investigated the anti-inflammatory response from exogenous itaconate in S100-induced AIH, and our results showed that itaconate treatment attenuated liver histopathological damage, hepatocyte apoptosis, aminotransferase elevation, and IL-6 production in the S100-induced AIH model. In addition, Itaconate decreased glycolysis to suppress the maturation of DCs in the liver and spleen of AIH models, thereby directly regulating differentiation of Th17 and Tregs *in vivo*. The percentage of Th17 cells among the CD4⁺ population were decreased and Tregs were increased ($P < 0.05$). Furthermore, Itaconate-induced bone marrow-derived monocytes suppressed CD4⁺ cells proliferation. *In vitro* and *in vivo*, we found that itaconate suppressed autophagy via activating the PI3K/AKT/mTOR signalling pathway in bone marrow-derived DCs and liver tissues. We further investigated the function of Itaconate on DC-specific mTOR-deficient mice. mTOR-deficient DCs augmented inflammatory reactions in mTOR^{DC-/-} AIH mice and induced autophagy. MHY1485 (an agonist of mTOR) and itaconate significantly alleviated the inflammatory reaction and autophagy signalling. In conclusion, itaconate ameliorate liver inflammation in S100-induced AIH mice by regulating the PI3K/AKT/mTOR pathway to decrease DCs autophagy and maturation. These results provide insight useful for treating AIH.

* Corresponding author. Department of General Surgery, The First Hospital of Lanzhou University, Lanzhou, NO.1 Donggang West Road-Gansu, 730000, China.

E-mail address: lix@lzu.edu.cn (X. Li).

<https://doi.org/10.1016/j.heliyon.2023.e17551>

Received 24 January 2023; Received in revised form 14 June 2023; Accepted 20 June 2023

Available online 22 June 2023

2405-8440/© 2023 The Authors. Published by Elsevier Ltd. This is an open access article under the CC BY-NC-ND license (<http://creativecommons.org/licenses/by-nc-nd/4.0/>).

1. Introduction

Autoimmune hepatitis (AIH) is an immune-mediated chronic inflammatory response against liver cells characterized by interface hepatitis, elevated aminotransferase levels, increased autoantibody levels, and an imbalance in regulatory T (Treg)/Th17 cells [1,2]. During dysregulation of immune homeostasis, the main underlying pathogenetic mechanism of AIH is abnormal T cell-mediated responses to autologous hepatocytes [3]. Dendritic cells (DCs) are pivotal master initiators of the antigen-specific immune response. Immunogenic DCs promote the expansion and differentiation of effector T cells to protect against pathogens and autoantigens, whereas tolerogenic DCs (tol-DC) instruct Tregs to dampen autoimmunity and prevent chronic inflammation. Breakdown of DC-mediated tolerance is closely linked with the pathological progress of AIH. Intracellular metabolic changes in the immune system promote effector mechanisms in the immune response [4]. The activation and effector function of DCs are dependent on reprogramming of intracellular metabolic pathways [5]. Improving the understanding of that itaconate regulates DC effector functions and immune response in S100 induced-liver inflammation may provide insight into the causes of and therapeutic strategies for AIH.

Inflammatory activation of DCs impairs mitochondrial respiration and disrupts the tricarboxylic acid cycle, leading to the accumulation of endogenous metabolites that may adopt immunomodulatory roles. Itaconate, produced from citrate, is one of the most abundant metabolites in activated Macrophages, and has broad immunosuppressive properties. Multiple physiological metabolites in macrophages have exhibited immunoregulation properties and exerted protective effects in various disease models [6]. Itaconate and its derivatives have been successfully applied as an immunoregulatory effector in the treatment of inflammatory diseases, including ulcerative colitis, liver ischemia reperfusion, systemic lupus erythematosus, and systemic sclerosis [7–11]. Itaconate exerts anti-inflammatory effects via many pathways [12,13], including by attenuating the inflammatory response in stimulated macrophages by impairing glycolysis [14,15]. Itaconate is encoded by immune-responsive gene 1 (*Irg-1*), the expression and peak levels of which vary under different conditions in inflammation and autoimmune diseases [16]. The cellular response to itaconate may differ by cell type. Recent research found that the *Irg-1*/Itaconate pathway is a vital determinant of DC's immune-priming function and contributes to resolve house dust mite-induced asthma [17]. Therefore, the role of itaconate on DCs in the pathogenesis of AIH should be evaluated. The mechanisms and pathways involved in these effects were also examined. The ability of itaconate to mediate immunosuppression may be useful for treating AIH. Our findings confirmed that the activation of the *Irg-1*/Itaconate-pathway is involved in liver inflammation in AIH. We hypothesized that itaconate alleviates liver inflammation by regulating DC immune function.

1.1. In this study, we investigated the immunomodulatory

Effects of exogenous Itaconate on DC activation and liver inflammation in a homologous liver autoantigens (S100)-induced mouse AIH model. The results showed that exogenous itaconate could alleviate liver histopathological damage, hepatocyte apoptosis, lymphocyte infiltration, and IL-6 production. Itaconate suppressed maturation of DC and induced DC immune tolerance by inhibiting CD4⁺ T cells proliferation and Tregs generation *in vivo* and *in vitro*. Furthermore, itaconate modulated DCS function by blocking DCs autophagy. Our findings further deeply reveal the mechanisms and pathways regulated by Itaconate and provide a new useful approach for AIH treatment.

2. Materials and methods

2.1. Animals

Six- to eight-week-old male C57BL/6 mice were obtained from Lanzhou Veterinary Research Institute. The conditional knockout mouse bearing floxed mTOR with a CD11c-Cre deletion strain (mTOR^{DC-/-}) was obtained from the Institut Pasteur of Shanghai Chinese Academy of Sciences. All mice were housed in a specific-pathogen-free (SPF) facility Laboratory Animal Center with controlled temperature (24 ± 2 °C) and humidity. The mice received standard laboratory chow and water. All animal experiments conformed to the animal care protocols by the Ethics Committee of the Lanzhou University NO1 Hospital, China (the approved protocol number for animal experimentation: LDYLL-2022-334).

2.2. AIH model

The allogeneic C57BL/6 male mice were anesthetized by intraperitoneal injection with 0.004 mL/g 10% chloralhydrate. The liver homogenate was freeze-thawed at -80 °C and 37 °C three times and the supernatant was centrifuged at ultra-high speed (100 000×g) for 1 h. The S100 liver antigen subcomponents were separated from the final supernatant by a 90 cm Cl-6B Sepharose column. Hereinafter, the S100 protein subcomponent combined with Freund's adjuvant (Sigma-Aldrich St. Louis, MO, USA) is referred to as S100. In this experiment, the concentration of S100 used was 2.0 g/L. Next, the C57BL/6 mice and mTOR^{DC-/-} mice were intraperitoneally injected with 2.0 g/L of S100 on day 7 and 21. Mice were randomly divided into groups: the normal control (NC) group (n = 6); the model group (AIH) treated with S100 (n = 6); and the treatment group (AIH + ITA) treated with Itaconate obtained from Sigma-Aldrich (St. Louis, MO, USA) (n = 6), the treatment group (mTOR^{DC-/-} + MHY) treated with MHY1485 (Abmole, Houston, USA). After mice were euthanized at day 42, the liver and spleen were taken, photographed and weighed to observed the changes of spleen in size and weight.

2.3. Determination of itaconate by LC-MS

For targeted metabolite analysis, extracts were analysed using a triple quadrupole TSQ Quantum mass spectrometer coupled to an UltiMate 3000 RS chromatograph (Thermo, Massachusetts, USA) in Wuhan Servicebio Technology Co., Ltd. Freeze-dried mouse liver samples were added to methanol to extract metabolites. Detection method: select reaction monitoring (SRM). Under the same conditions, the chromatogram of the sample was compared to the standard chromatogram of itaconic acid, and the chromatographic peaks of each component in the sample were determined according to retention time. All chromatogram data of itaconic acid was processed and integrated using the software, Xcilabur 3.0 (Thermo, Massachusetts, USA), and quantitation was achieved by linear regression with weighted coefficients.

Table 1
The severity of AIH mice model.

	NC(n = 6)	AIH(n = 6)
Ascites	no	more
Liver texture	Soft, smooth	Tough, fibrosis
Spleen size	normal	splenomegaly
Mortality	0/6	3/6
Weight(g)	26.8 ± 1.9	22.5 ± 2.3**
HE scores	0.5 ± 0.29	2.75 ± 0.25**

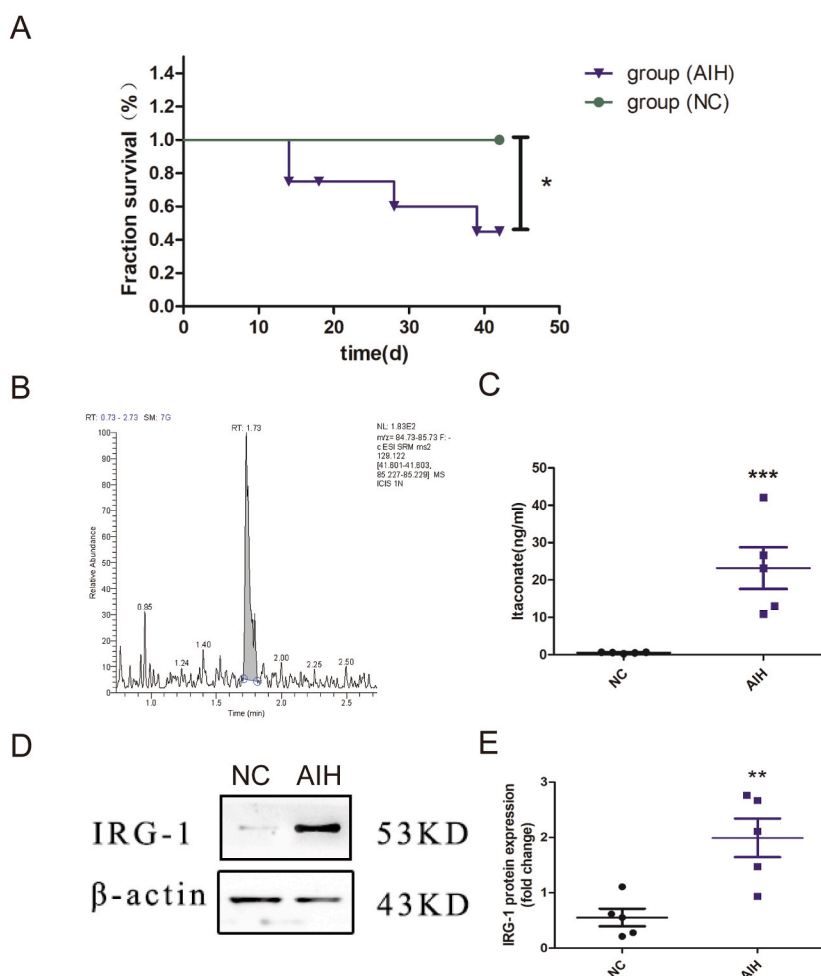
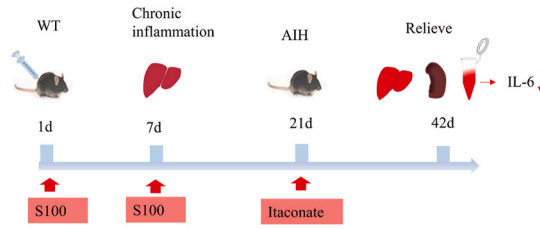


Fig. 1. IRG-1/Itaconate pathway was altered in S100-induced AIH mice. (A) The survival curves of mice in indicated groups (data were collected every 6 days; n = 8 for each group). (B) Typical total ion flow chromatogram of endogenous itaconate in the liver tissue samples measured by liquid chromatography-mass spectrometry analysis. (C) Quantitative analysis of the value of itaconate in different groups. (D) The protein expression of IRG-1 was determined by western blotting. (E) The quantitative analysis of the expression of IRG-1, the relative protein levels were normalized to β -actin. * = $p < 0.05$, ** = $p < 0.01$ and *** = $p < 0.001$.

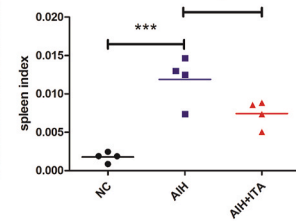
A



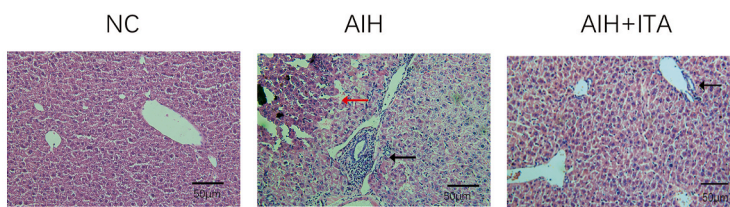
B



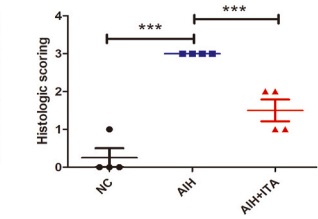
C



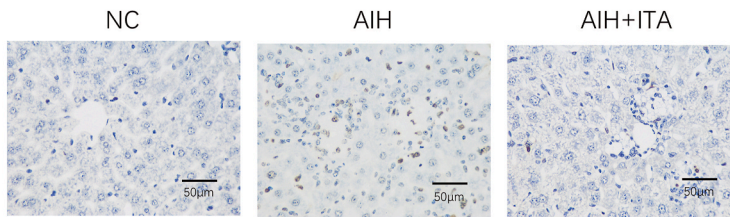
D



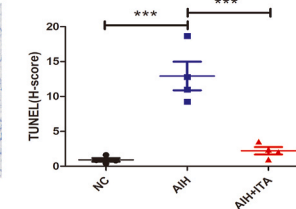
E



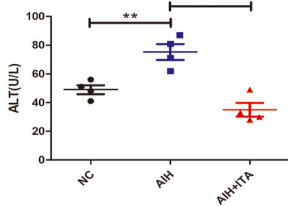
F



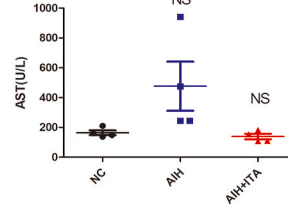
G



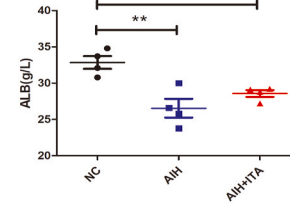
H



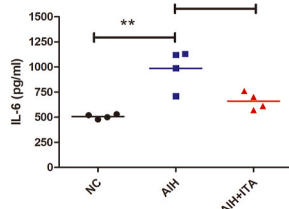
I



J



K



(caption on next page)

Fig. 2. Exogenous itaconate alleviated liver injury in mice with S-100-induced AIH. (A) Schematic showing the experimental design and treatment of S100 induced-mouse AIH model. Model group mice were intraperitoneally injected with S100 (0.5ml/mice) on day1 and 7; On day 21, the treatment group (AIH + ITA) was intraperitoneally administered 50 mg/kg itaconate. While the NC and model groups (AIH) received an equivalent volume of phosphate-buffered saline, (B) Representative images of liver and spleen tissues (scale bar = 1 cm) in indicated groups. (C) The index of spleen (the ratio of weight of spleen and weight of body) were compared. (D) Representative images of haematoxylin and eosin (scale bar = 50 μ m), and assessed for the severity of hepatitis by two pathologists in a blinded manner. The black arrows highlight lymphocytic infiltration. The red arrows highlight hepatocyte necrosis (magnification: \times 200). (E) Quantitative analysis of the liver damage. (F) TUNEL staining indicated apoptotic hepatocytes (scale bar = 50 μ m); positive cells with brown nucleus were counted in three fields. (H–J) ALT, AST and ALB in the serum. (K) Serum IL-6 levels. N = 4, Data are presented as mean \pm SD of three independent experiments. * P < 0.05, ** P < 0.01 and *** P < 0.001. NC, normal control; AIH, Autoimmune hepatitis; ITA, Itaconate; IL-6, interleukin-6; ALT, alanine aminotransferase; AST, aspartate transaminase; ALB, albumin. (For interpretation of the references to colour in this figure legend, the reader is referred to the Web version of this article.)

2.4. Energy metabolomics

The intracellular energy metabolites were analysed by Liquid chromatography-tandem mass spectrometry (LC-MS/MS) analysis in Shanghai Applied Protein Technology Co. Ltd. The sample (1×10^7 DC cells were isolated from spleens of each group) were taken out at -80 °C. Then 400 μ L of cold methanol/acetonitrile (1:1, v/v) was added to remove the protein and extract the metabolites. LC analysis was performed using a 1290 Infinity LC system (Agilent, California, USA). Mass spectra acquisition was performed using a 5500 QTRAP mass spectrometer (AB SCIEX, USA) on negative ionization mode and MRM mode. The energy metabolite standard was used to correct the retention time and identify metabolites. Peak areas and retention times were analysed using Multiquant software.

2.5. Liver function and cytokine assay

Retro-orbital blood samples were collected from mice and centrifuged at $1000 \times g$ for 15 min to separate plasma. The levels of alanine aminotransferase (ALT), aspartate transaminase (AST), and albumin (ALB) were determined using an automatic dry biochemical analyser (AU5800, Beckman Coulter, USA) from the Clinical Laboratory Department of the First Hospital of Lanzhou University. The levels of IL-6 in murine plasma were analysed using ELISA kits (DAKEWE, Shen Zhen, China), according to the manufacturer's instructions.

2.6. Liver histological assessment

Liver tissues from the mice were fixed in 10% formalin. After paraffin embedding, sections were dewaxed and rehydrated. The slices were stained with haematoxylin-eosin (H&E) and immunohistochemical stain incubated with 1st and 2nd antibodies. The brown cell areas were observed under microscopy (Nikon, E100, Tokyo, Japan) and calculated with an image system (Nikon DS-U3, Tokyo, Japan). The liver damage score was evaluated by two independent and experienced pathologists, adopting the revised Kondell protocol [18].

2.7. TUNEL assay

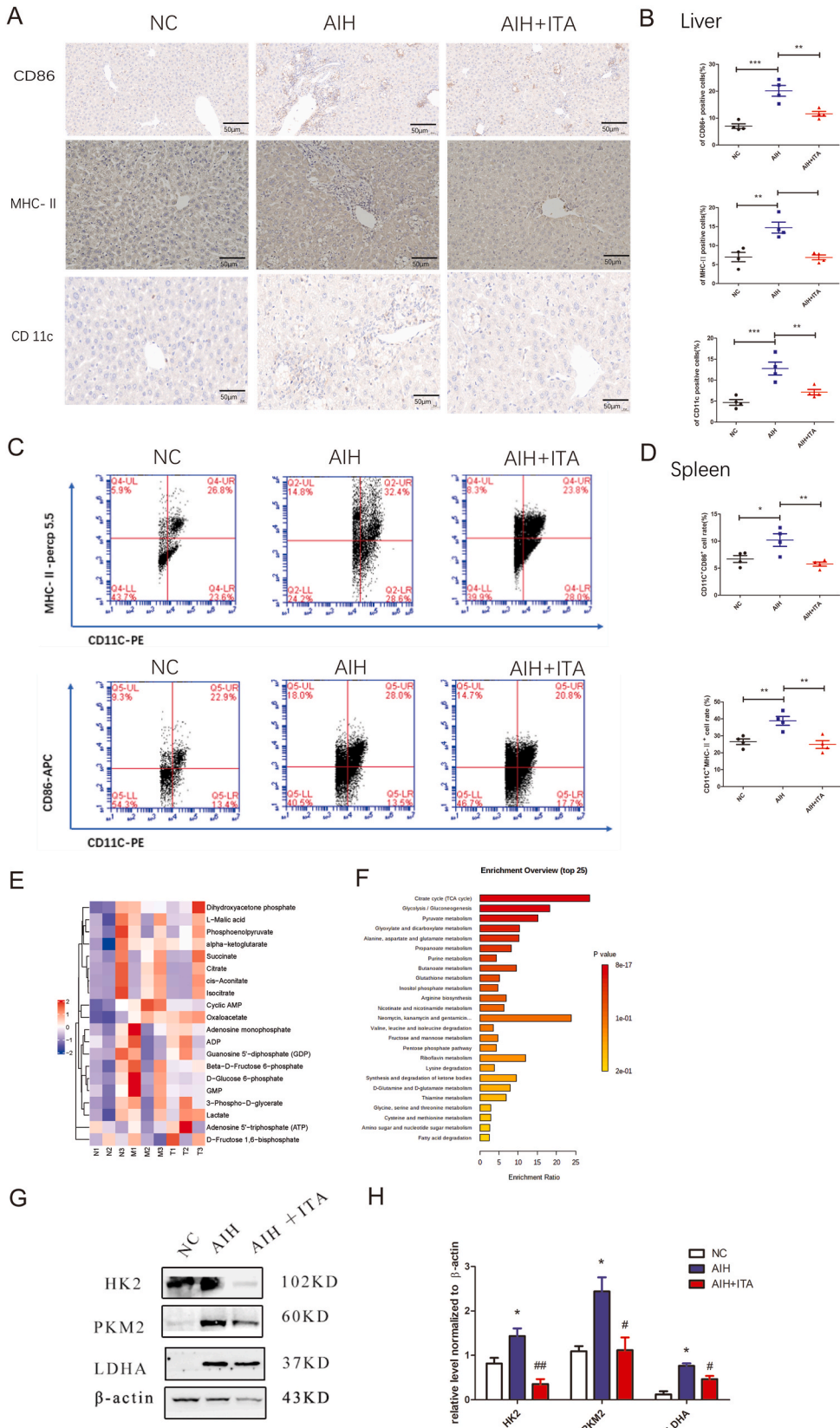
The TUNEL assay was carried out with the TUNEL kit (G1507, Servicebio, China) as instructed by the manufacturer. Liver sections (5 μ m thickness) embedded in paraffin were dewaxed and dehydrated, and then incubated with TUNEL reaction mixture at 37 °C for 1 h. Finally, the tissues were labelled with DAB chromogenic agent and observed via light microscopy.

2.8. Flow cytometry analysis

To obtain single cell suspension, the spleen tissues collected from mice were grinded and filtered. The red blood cells were lysed with Red Blood Cell Lysing buffer (Sigma-Aldrich, USA). The freshly prepared lymphocytes (1×10^6) were suspended in 100 μ L PBS and stained with the following different combinations of fluorescent-coupled antibodies obtained from Biolegend (San Diego, CA, USA): PE-anti-mouse CD11c, Percp 5.5-anti-mouse MHC-II, APC-anti-mouse CD86. To detect Th17 and Treg cells, T cells were stimulated with the PMA/Ionomycin and BFA/Monensin (CS1001, Multi Science, China) mixtures for 5 h; cells were collected and stained with Percp 5.5-anti-mouse CD4 and PE-anti-mouse CD25, respectively. T cells were incubated with fixation and permeabilisation diluent (Invitrogen, Carlsbad, California, USA). Then T cells were further stained with APC-anti-mouse IFN- γ , PE-anti-mouse IL-17, FITC-anti-mouse Foxp3. The above antibodies were obtained from Biolegend (San Diego, CA, USA). Data were acquired via flow cytometry on a Fluorescence-activated cell sorter (FACS; BD Accuri C6) and analysed using BD Accuri C6 software.

2.9. Cell purification and culture

Bone marrow-derived monocytes (BMDC) were isolated from mouse femur and tibial bone marrow and cultured *in vitro* with culture medium containing 10% FBS, recombinant mouse 40 ng/mL GM-CSF and 40 ng/mL IL-4 (ProteinTech, Chicago, USA). Later, BMDCs were stained with PE-CD11c microbeads (130-108-338, Miltenyi Biotec, Bergish Gladbach, Germany), and positively sorted via magnetic cell sorting (Auto-MACS-Pro, Miltenyi, Germany). At the same time, naïve CD4⁺ T cells were positively sorted from



(caption on next page)

Fig. 3. Exogenous itaconate regulated the proportion and maturation of DCs *in vivo*. (A, B) IHC staining and Quantitative analysis of CD86, MHC-II and CD11c in the hepatic tissues of indicated groups (Original magnification:x200). (C, D) Representative plots and quantification of flow cytometry for surface costimulatory molecules of DCs in the spleen tissues of indicated groups. The data represent the mean \pm S. D from four experiments. (E) DCs isolated from the spleen were analysis by energy metabolomic. Heat maps showing different abundant metabolite features in spleen DCs of indicated groups, with enriched metabolites were highlighted in red.(F) Bar graph shows top 25 metabolic pathways distinctly perturbed by itaconate treatment, Bar length relates to the pathways of different expressed metabolite sets. (G,H)Representative western blotting images and the relative expression of glycolysis associating proteins, HK2, PKM2, and LDHA in indicated groups; * $P < 0.05$, ** $P < 0.01$ and *** $P < 0.001$ vs control. NC, normal control; AIH, Autoimmune hepatitis; ITA, Itaconate; N, normal control; M, model group treated with S100; T, treat group with itaconate; HK2, Hexokinase 2; PKM2,Pyruvate; LDHA, Lactate dehydrogenase. dehydrogenase 2; LDHA, Lactate dehydrogenase; KD, kilodalton. (For interpretation of the references to colour in this figure legend, the reader is referred to the Web version of this article.)

lymphocytes of the spleen from allogeneic mice using MACS CD4 MicroBeads (130-117-043, Miltenyi Biotec, Bergish Gladbach, Germany), and cultured with mouse lymphocyte culture medium in the presence of soluble anti-mice CD3/CD28 monoclonal antibody and IL-2 (5 $\mu\text{g}/\text{mL}$) *in vitro*. The purified BMDC was further used in co-culture and adoptive transfection experiments.

2.10. Mixed lymphocyte reaction

Activated DCs treated with different agents were plated into a 24-well plate, co-cultured with allogeneic naïve CD4+T cells, which were previously labelled with 0.5 μM carboxyfluorescein succinimidyl ester (CFSE) (Sigma-Aldrich St. Louis, MO, USA), in the presence of 5 $\mu\text{g}/\text{mL}$ soluble anti-mice CD3/CD28 monoclonal antibody at a ratio of 1:5 (DC/T cell) for 3 days. To investigate the role of BMDC on the proliferation of CD4+T cells, the collected T cells were stained with anti-mouse CD4 after co-cultivation. The fluorescence intensities of CFSE dye on CD4+T cells were detected on a BD C6 flow cytometer by the FL1 (FITC) channel.

2.11. Monodansylcadaverine (MDC) staining

Autophagic vacuoles were detected by MDC (Solarbio, Beijing, China) staining. BMDCs were seeded in 24-well plates with a density of 1×10^5 cells/well, and then treated with saline or S100 (20 $\mu\text{g}/\text{mL}$) alone or in combination with itaconate or chloroquine (Selleck, Houston, USA) for 12 h. Next, cells were incubated with an appropriate amount of preheated working solution containing MDC probe (50 μM) for 30 min in the dark at 37 °C. Autophagic vacuoles formed in the cells were detected under fluorescence microscopy.

2.12. Western blot

Total protein was extracted from the liver tissues of mice or BMDC using a mixture of RIPA lysis buffer, phenylmethanesulfonyl fluoride (PMSF, Beyotime Biotechnology, Haimen, China) and phosphatase inhibitors. Equivalent amounts of total proteins were separated via 6 or 10% sodium dodecyl sulfate-polyacrylamide gel electrophoresis (SDS-PAGE) and transferred onto polyvinylidene fluoride (PVDF) membranes (Millipore Corp, Billerica, MA, USA). After blockade with 5% BSA for 1 h, membranes were incubated with primary antibodies overnight at 4 °C, and the blots were incubated with secondary antibody at 37 °C for 2 h. As an internal control, β -actin was detected using an anti- β -actin antibody, and the immunoreactive bands were analysed using Fluorochem FC3 (ProteinSimple, USA) chemiluminescence system. Detailed information about antibodies can be found in the KEY RESOURCES TABLE of [Supplementary Table 1](#).

2.13. Statistical analysis

GraphPad Prism 8 (La Jolla, CA, USA) was used for all statistical analyses and generation of plots. All data are presented as the mean \pm SE. Intergroup comparisons of the quantitative data was analysed by one-way analysis of variance (one-way ANOVA). Multiple comparisons of the means of two samples were performed using independent-samples t-tests, and the correlations between two variables were assessed using Pearson correlation analysis. Survival was analysed using Kaplan-Meier log-rank test. $P < 0.05$ was considered statistical significance. No data exclusions were made in experimental sections. The main statistical parameters (F, t, exact p values and N/group) are in a [Supplementary Table 2](#).

3. Results

3.1. IRG-1/itaconate pathway was altered during AIH

To explore the immunomodulatory effects of the IRG-1/Itaconate-pathway in AIH, we employed the homologous hepatic auto-antigen S100-induced AIH model that successfully mimicked liver injury in human AIH ([Supplementary Figs. 1A–D](#)), which is useful for evaluating the pathogenesis of autoimmune hepatitis [19]. We found that S100 increased the mortality and severity of AIH ([Table 1](#)) and decreased the total survival time ([Fig. 1A](#)) of the model mice. We assumed that endogenous itaconate production and IRG-1 expression by liver might be due immune response in S100-induced AIH. Itaconate production assessed using targeted liquid chromatography–mass spectrometry (LC-MS) were significantly increased in AIH ([Fig. 1B](#) and C), and was correlated with upregulation of IRG-1 ($P < 0.01$) ([Fig. 1D](#) and E), which mediates the decarboxylation of *cis*-aconitate to itaconate. These findings demonstrate

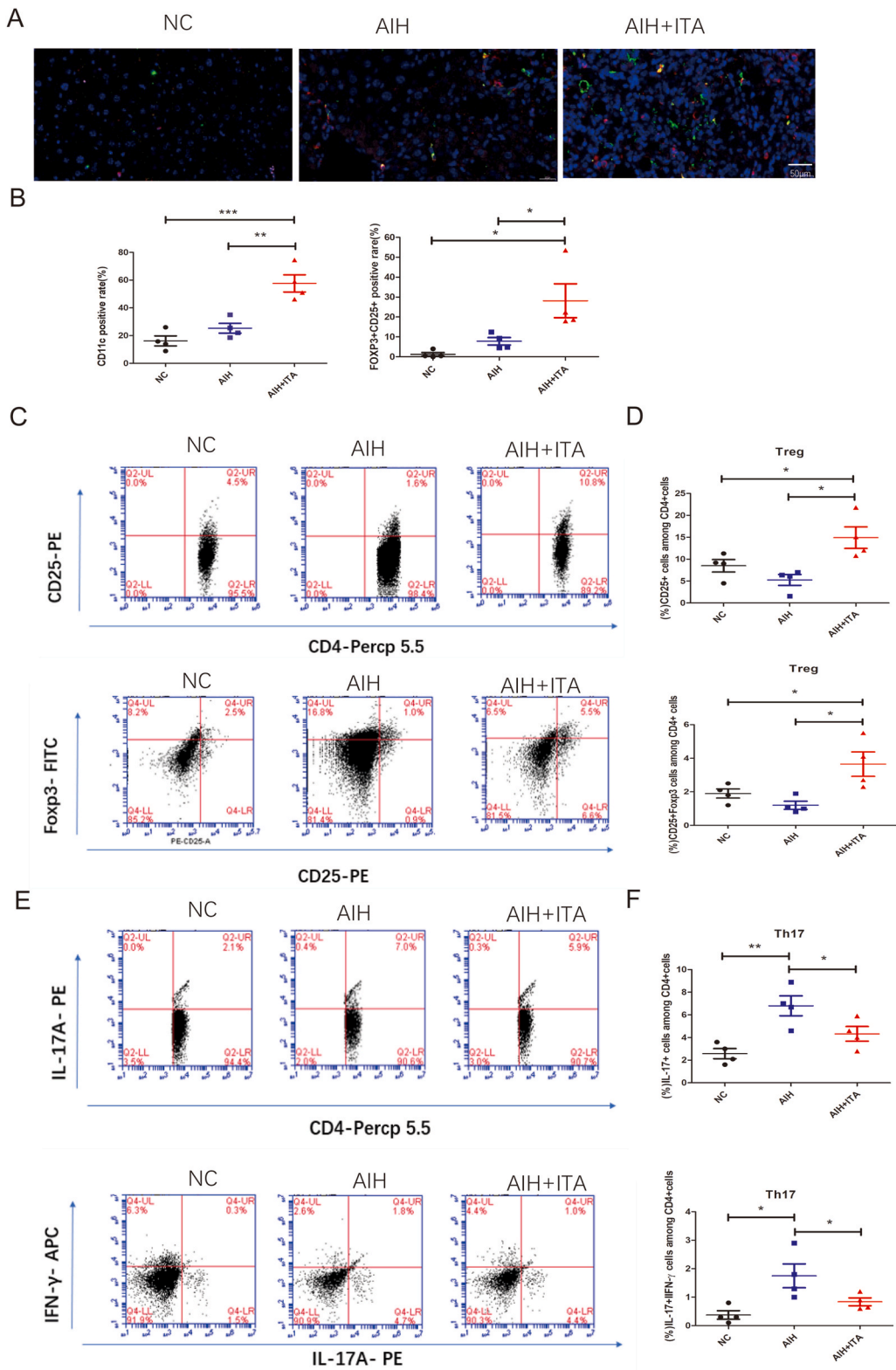


Fig. 4. DC modulated Th17 and Treg differentiation during S100 induced-AIH. (A) DC and Treg cells infiltration in the liver tissues of different groups were analysed via immunofluorescence (IF). Canonical CD11⁺MHC-II⁺DCs infiltrate in the liver of mice were stained for CD11c- Cy5 (pink), Treg cells were stained for CD25-Cy3 (red) and Foxp3-FITC(green). Treg Cells expressing both appear in yellow. (B) Quantitative analysis of the value of DCs and Treg cells; (C,E) Typical CD4⁺CD25⁺Foxp3⁺ Tregs cells and CD4⁺IL17⁺IFN-γ Th17 cells in spleen were determined via flow

cytometry analysis and quantitative analysis in different groups (D,F). Results are depicted as mean \pm SD and were repeated thrice independently. * $P < 0.05$, ** $P < 0.01$ and *** $P < 0.001$. NC, normal control; AIH, Autoimmune hepatitis; ITA, itaconate; Tregs, Regulatory T cells. (For interpretation of the references to colour in this figure legend, the reader is referred to the Web version of this article.)

that the activation of the IRG-1/Itaconate-pathway is involved in liver inflammation in AIH.

The homologous hepatic autoantigen S100-induced AIH model. In the AIH group, after injected the S100 solution, the texture of liver became fibrosis and tough, while the size of spleen became larger. The mice exhibited more ascites, declined weight trend, higher mortality, compared to the NC group. The liver exhibited substantially increased histological severity of hepatitis, compared with NC group ($P < 0.01$).

3.2. Exogenous itaconate alleviated liver injury in AIH mice

To support the view that itaconate has a potential anti-inflammation biological function, we evaluated whether exogenous itaconate *in vivo* might ameliorate liver inflammation in S100-induced AIH mice (Fig. 2A). The spleen size and spleen index were significantly lower in mice receiving itaconate compared with S100-treated mice (Fig. 2B and C), and histological analysis showed that itaconate reduced the extent of liver tissue necrosis and lymphocyte infiltration ($P < 0.001$) (Fig. 2D and E). We also found that there was a negative correlation of itaconate with liver H&E score (Supplementary Fig. 2A). TUNEL assay analysis of hepatocyte apoptosis indicated that areas positive for apoptotic cells in the itaconate-treated group decreased significantly ($P < 0.01$) (Fig. 2F and G). Histopathological examination and the levels of ALT were used to assess the liver damage. We found that itaconate decreased ALT and increased ALB levels compared with the S100-treated group (Fig. 2H and K), although aspartate aminotransferase (AST) levels were not significantly changed (Fig. 2I). Serum IL-6, an important inflammatory factor secreted by hepatic cells, was significantly suppressed following itaconate treatment compared to that in the AIH group (Fig. 2K). These results support that exogenous itaconate treatment attenuated liver inflammation and hepatocyte injury.

3.3. Exogenous itaconate diminished the proportion and maturation of DCs *in vivo*

DCs play an important role in activating adaptive immunity and promoting immune tolerance. Breakdown of the tolerance of DCs is closely linked with the pathogenesis of AIH [20]. First, we investigated the characteristics of DCs in the liver tissues using immunohistochemistry. We confirmed the tolerance function of intrahepatic DCs treated with itaconate; DCs with lower expression of MHC-II and CD86 infiltrated the portal areas in the liver with itaconate treatment but not in that with S100 treatment (Fig. 3A and B), indicating that itaconate inhibited DC antigen presentation to T cells. To determine whether the maturation state of spleen-derived DC differs from DCs in the liver tissue, we performed flow cytometry to analyse maturation marker expression on spleen DCs. Similarly, the expression of costimulatory molecule CD86 and MHC-II in CD11c⁺DCs in the itaconate-treated group was decreased ($P < 0.01$) (Fig. 3C and D), indicating that itaconate induced tol-DC production *in vivo*. To further verify this hypothesis, we generated bone marrow-derived DCs (BMDCs) and cultured the cells with S100 or itaconate (20 mg/mL) from days 6 to 8. The results were the same (Supplementary Figs. 5A–C). Occurrence of immune tolerance and the immune response in DCs depend on reprogramming of intracellular metabolic pathways [21]. Itaconate induced tol-DCs partly by altering immune cell metabolism. The energy metabolite set enrichment analysis showed that the metabolic pathways switched from glycolysis to oxidative phosphorylation when DCs were stimulated via itaconate (Fig. 3E and F). Oxaloacetate, the intermediate metabolite of tricarboxylic acid cycle, was significantly upregulated by itaconate stimulation compared to that in S100 pulsed DCs (Supplementary Fig. 3A). We next investigated the expression levels of glycolysis-associated proteins in the liver tissues and found that the expression levels of the glycolytic enzymes HK2, LDHA, and PKM2 were downregulated in the itaconate-treated group ($P < 0.01$) (Fig. 3G and H). Collectively, these data suggest that itaconate promotes DC immune tolerance by inhibiting DC glycolysis in S100-induced AIH mice.

3.4. DCs modulated the differentiation of Th17 and Treg during S100 induced-AIH

As tol-DCs induces Tregs to dampen autoimmunity, we investigated Tregs and Th17 cells in the liver and spleen to determine whether DCs modulate T cell differentiation following itaconate stimulation. DC and Treg cell infiltration in the livers were analysed using immunofluorescence. With an increasing proportion of CD11c^{high}DC cells, the frequency of Tregs (CD25⁺Foxp3⁺) was significantly increased (Fig. 4A and B). Similarly, flow cytometry analysis revealed that S100 treatment increased the percentage of Th17 cells (Supplementary Fig. 4A) among the CD4⁺ population and decreased Treg cells (Supplementary Fig. 4B) in the spleen (Fig. 4C and D), whereas itaconate treatment reversed these changes (Fig. 4E and F). Thus, increased Tregs may promote CD4⁺T cell immune tolerance. These results confirm that itaconate treatment induced DC tolerance, which can lead to no or low reactivity of T cells and promote the differentiation of native T cells towards Treg cells.

3.5. Itaconate-induced BMDCs suppressed CD4⁺ proliferation *in vitro* and protected against hepatic injury

Tregs are important for maintaining immune tolerance in the body. Tol-DCs induce Tregs generation through cell-cell contact-dependent signalling, secretion of targeted proteins and cytokines, as well as other mechanisms [22]. To investigate whether DCs regulate T cell proliferation directly *in vitro* and *in vivo*, we cultured the BMDCs with S100 or Itaconate (20 mg/mL) from days 6 to 8

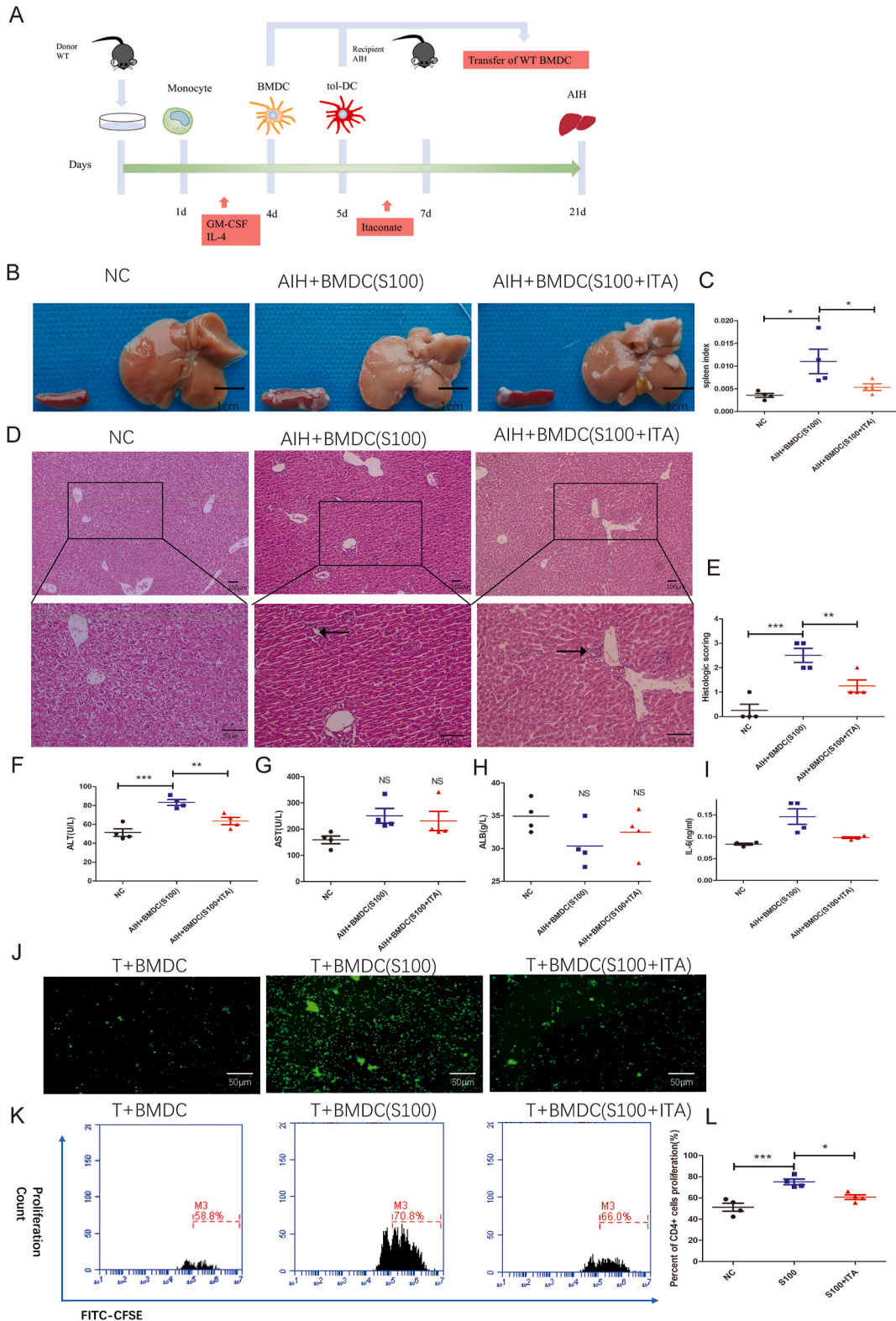


Fig. 5. Treatment of BMDCs with Itaconate inhibited CD4⁺ T cell proliferation *in vitro* and protected against hepatic injury. (A) Induction and culture schema of BMDCs and cell transplantation. BMDCs from WT mice were cultured with GM-CSF and IL-4, then stimulated with S100 in the presence or absence of itaconate for 48 h and were injected into AIH mice via tail-quietly. (B) Representative images of liver and spleen tissues (scale bar = 1 cm) in indicated groups. (C) The index of spleen. (D, E) Representative H&E staining micrographs (scale bar = 50 μm) and quantitative

analysis of the liver inflammation. Black arrows highlight lymphocytic infiltration. (F–H) ALT, AST and ALB in the serum. Data were expressed as the mean \pm SD (n = 4). (I) Serum concentrations of IL-6 (G) Representative photographic images of CD4⁺T cell proliferation labelled with CFSE and observed under a fluorescence microscope. (J, K) Quantification of percent proliferation in indicated groups, using flow cytometry analysis (n = 4 biological replicates). *P < 0.05, **P < 0.01 and ***P < 0.001. BMDC, Bone Marrow-derived dendritic cell; GM-CSF, Granulocyte macrophage colony stimulating factor; IL-4, interleukin 4; Tol-DC, tolerogenic dendritic cells.

(Supplementary Fig. 5A), and transferred the BMDCs into AIH C57BL/6 recipient mice (Fig. 5A). We found that the spleen index was reduced, hepatocyte necrosis and inflammatory cell infiltration were reduced, and the levels of ALT and IL-6 were significantly decreased in recipient AIH mice receiving the itaconate-induced BMDC compared with S100-induced BMDC (Fig. 5B–D). Further, the results of coculture experiments showed that S100-induced BMDCs exhibited promoting CD4⁺ T cells proliferation. In contrast, treatment of BMDCs with itaconate inhibited CD4⁺ T cells proliferation (P < 0.05) (Fig. 5G–L) and potentiated the conversion of effector cells into Tregs (data not shown). These *in vitro* results show that itaconate directly affected DCs activity and influenced the proliferation of CD4⁺T cells by altering cell-to-cell communication, resulting in anti-AIH effects *in vivo*.

3.6. Itaconate inhibited BMDC autophagy through the PI3K/AKT/mTOR pathway in S100-induced AIH mice

To confirm whether the alleviation of AIH by itaconate is associated with autophagy in DCs, we evaluated autophagy-related protein expression in BMDCs using western blotting. The protein levels of LC3-II/LC3-I and Beclin-1 were upregulated following treatment with S100, whereas itaconate reversed these effects (Fig. 6A and B). To confirm that these results were related to autophagy flux, we used the autophagy inhibitor chloroquine, which prevents fusion between autophagosomes and lysosomes. LC3-II levels were downregulated in the presence of chloroquine. Thus, itaconate decreased autophagy by impairing autophagy flux rather than by blocking the autophagy pathway. Next, we performed *in vitro* labelling of late-stage autophagic vacuoles in BMDCs to monitor the effect of itaconate on autophagy. Fewer MDC-labelled vacuoles accumulated in the cytoplasm of BMDCs in the itaconate-treated group (Fig. 6D). Autophagy-related protein expression in the liver tissues treated with itaconate was consistent with the results observed *in vitro* (Fig. 6E and F). The overall effect of mTOR on autophagy was mainly determined by the autophagy axis itself; the mediation of autophagy in BMDCs is regulated by mTOR signalling (Fig. 6C). *In vivo*, the phosphorylates levels of p-AKT/AKT and p-mTOR/mTOR were significantly decreased in the S100-treated group and increased in the itaconate-treated groups (P < 0.05) (Fig. 6G and F). mTOR exists as two supramolecular complexes (mTORC1 and mTORC2). p-S6 is indicative of mTORC1 activity. mTORC1 directly phosphorylates the effect of protein p70s6 kinase 1 and 4E-BP-1 to initiate translation of distinct mRNAs [23]. We found that itaconate treatment *in vivo* significantly increased the levels of phosphorylated p70S6, S6, and 4E-BP-1 (Fig. 6I and J). These results indicate that autophagy dysfunction is ameliorated by Itaconate via recovery of the PI3K/AKT/mTOR signalling pathway.

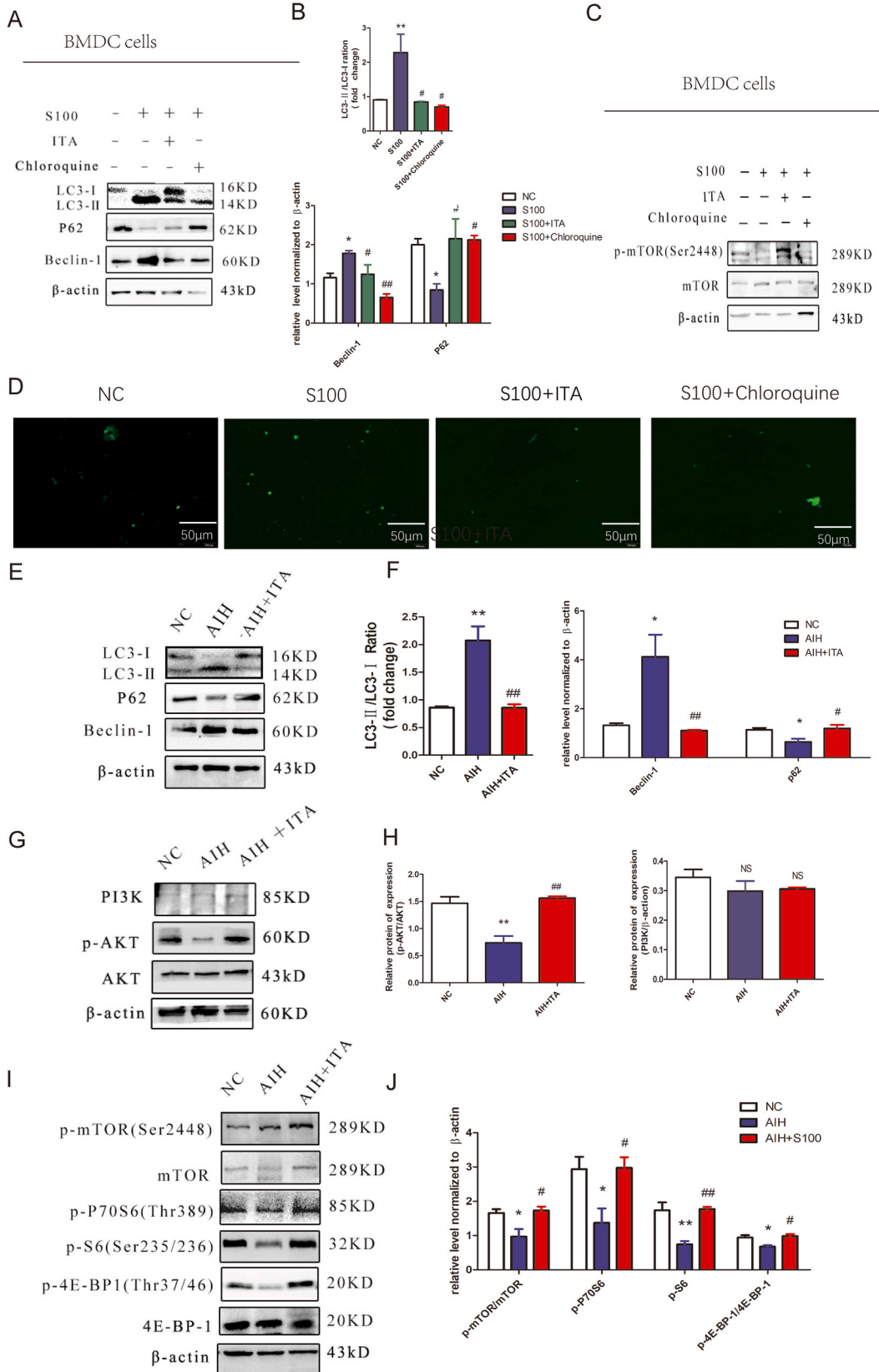
3.7. Itaconate alleviated liver inflammation and inhibition autophagy in mTOR^{DC-/-} AIH mice through mTOR signalling

To investigate how immune responses regulated by the mTOR signalling pathway affect DC function, we bred mice with mTOR-specific knockout of DCs (CD11C-cre-mTOR-floxed, mTOR^{DC-/-}). The results showed specific genetic ablation of mTOR in DC cells (Supplementary Fig. 6A). The results showed that spleen size, spleen index, and portal areas lymphocyte infiltration and hepatocyte necrosis were exacerbated in mTOR^{DC-/-} AIH mice (P < 0.05) (Fig. 7A–D). mTOR-deleted DCs exhibited augmented proinflammatory cytokine production in mTOR^{DC-/-} AIH mice (Fig. 7E). We next performed a rescue experiment using mTOR^{DC-/-} AIH mice treated with MHY1485 (an agonist of mTOR) after S100 treatment. mTOR^{DC-/-}AIH mice administered MHY1485 showed reduced liver inflammation, and histopathological analysis indicated that the hepatocytes were preserved (Fig. 7C–E), which was as the same as itaconate. In addition, the expression levels of the autophagy-related proteins LC3-II and Beclin-1 showed an opposite trend: MHY1485 and itaconate blocked autophagy flux induced by S100 (Fig. 7F–H). In summary, itaconate alleviates liver injury in S100-induced mTOR^{DC-/-}AIH mice and reduce DC autophagy by regulating the mTOR signalling pathway.

4. Discussion

However, AIH is considered chronic hepatic damage, the mechanisms underlying the amelioration of AIH by itaconate remain unclear. S100 induced hepatitis has similar histopathology features and is suitable to establish AIH models. Our findings demonstrate that the activation of the IRG-1/Itaconate-pathway is involved in liver inflammation in AIH. Thus, itaconate may exert stimulus-dependent effects on inflammation. In addition, IRG-1-deficient mice showed an exacerbated inflammatory response [13,24], indicating that itaconate plays vital roles in this model. However, the endogenous production of itaconate was not sufficient to protect the liver damage. We found that exogenous itaconate as an immunomodulator, replenishing the endogenously-produced itaconate thereby preventing liver damage in S100-induced AIH mice. Our data highlight the protective effect of exogenous Itaconate in the AIH liver and suggest a therapeutic intervention.

Inflammatory cells play a key role in AIH-associated hepatic injury and the underlying mechanism was further investigated. DCs are the main cells maintaining the body's immune tolerance. Disrupting the balance of the immune response and tolerance regulated by DCs is closely related to the incidence of AIH [25]. Previous studies showed that the frequency of peripheral mature DCs was significantly increased in patients with AIH and experimental AIH mice and positively correlated with liver inflammation [26]. Similarly, our results demonstrated that the proportions of DCs and Tregs were increased after S100 administration, indicating



(caption on next page)

Fig. 6. Itaconate treatment exerts regulatory effects on BMDC autophagy via the PI3K/AKT/mTOR pathway in S100-induced AIH. (A) BMDC were cultured with normal medium, S100, S100+Itaconate, S100+Chloroquine respectively *in vitro*. (B) Protein expression of LC3, p62 and beclin-1 of BMDCs was measured via Western blot. (C) Protein expression of p-mTOR, mTOR of BMDCs was measured via Western blot. (D) Following each treatment, acidic vacuoles in BMDC cells were stained with MDC and observed under a fluorescence microscope. (E, F) Western blot and quantitative analyses of levels of LC3, p62 and beclin-1 in the liver tissues of AIH were measured via Western blot. (G, H) Western blot and quantitative analyses of levels of PI3K, p-Akt and Akt in the liver tissues of AIH mice were measured via Western blot. (I) Western blot for p-mTOR, mTOR, p-P70S6, p-S6, p-4E-BP-1 and 4E-BP-1 in liver tissues of indicated groups. β -actin was used as the internal control. (J) Quantitative analyses of protein levels showed that the p-mTOR/mTOR ratio as well as p-P70S6 and p-S6 of AIH + ITA group were upregulated compared with those of the AIH group. Values represent the mean \pm S. D of three experiments for each group. * $P < 0.05$, ** $P < 0.01$ and *** $P < 0.001$ vs control. # $P < 0.05$, ## $P < 0.01$ and ### $P < 0.001$ vs S100 or AIH. PI3K, phosphatidylinositol-3-kinase; AKT, protein kinase B; m-TOR, mechanistic target of rapamycin; KD, kilodalton.

proinflammatory DCs are related to the pathology of AIH. Tol-DCs are in an immature state and thus express low levels of costimulatory molecules (CD80/CD86) and MHC-II; they can phagocytose antigens but cannot effectively present antigens to T cells, and therefore cannot effectively activate T cells. Itaconate decreased the phenotypic maturity of DCs in the liver and spleen stroma. The occurrence of immune tolerance and the immune response in DCs depend on reprogramming of intracellular metabolic pathways. The activation, antigen presentation, migration, inflammatory factor secretion, and other biological processes of DCs are accompanied by profound changes in cellular metabolism. Tol-DCs are characterized by increased aerobic phosphorylation, decreased glycolysis, and lower IL-12 production [27]. Two recent studies revealed that negative feedback occurs between itaconate and glycolysis, which may be related to the anti-inflammatory effects of itaconate [14,15]. Analysis of energy metabolomics and glycolysis-related proteins showed that itaconate reduces glycolysis in DCs. These results support that itaconate exerts an immunosuppressive effect by decreasing glycolysis and inducing DC tolerance.

Tol-DCs can effectively induce Tregs production but not the Th1/Th17 response; this interaction may be a key link in the pathogenesis of autoimmune diseases [28]. Tol-DCs can induce immune tolerance by inducing T cell inactivation, apoptosis, and Tregs generation [29]. Inhibiting glycolysis in DCs downregulates the production of Th17 cells and facilitates Foxp3⁺Treg-mediated immune tolerance [30]. Tregs regulates the maturation and function of DCs by secreting IL-10 and TGF- β and downregulating the levels of MHC-II and costimulatory molecules [31]. Our results reveal DCs may modulate Th17 and Tregs differentiation via itaconate in S100-induced AIH. In addition, BMDCs induced by itaconate inhibited CD4⁺T cell proliferation *in vivo* and *in vitro*. Similar to direct application of itaconate in AIH mice, adoptive transferred itaconate-induced BMDCs alleviated liver inflammation and decreased serum IL-6 levels in AIH mice. IL-6 secreted by DCs reportedly plays a key role in controlling the balance of Th17 and Treg cells [32]. Taken together, we demonstrated that itaconate protects against T cell-mediated AIH, and its mechanism may involve regulation of the tolerance of DC-mediated differentiation of Tregs/Th17 cells.

Autophagy and apoptosis, known as programmed cell death processes, participate in the pathogenesis of AIH. Autophagy is a lysosomal degradation pathway that is critical to cytoplasmic homeostasis [33]. Numerous studies showed that autophagy is implicated in the progression of AIH. A recent clinical study demonstrated that abnormal autophagy is associated with extensive inflammation and an overactivated immune response [34]. Blockade of autophagy flux promoted the transformation of immunogenic DCs to tolerant DCs and decreased the proliferation of CD4⁺T cells [35]. Autophagy is implicated in the activation of adaptive immunity, promoting direct clearance of pathogens, antigen processing, and presentation to T cells [36]. In this study, S100 promoted autophagy on BMDCs; however, itaconate reversed these effects. In the cell experiments, chloroquine was used to verify the patency of autophagy flux. Our results indicate that Itaconate depressed autophagy by blocking the fusion of autophagosomes and lysosomes.

The precise regulation of autophagic flux by itaconate were further explored. The PI3K/AKT/mTOR signalling pathway is involved in the occurrence and development of AIH and appears to contribute to inflammation in dysfunctional autophagy [37]. PI3K/AKT is the upstream of the mTOR signalling pathway, and the AKT signalling pathway can downregulate autophagy [38]. A previous study revealed that pre-treatment with propylene glycol alginate sodium sulfate reduced hepatocellular apoptosis and autophagy by regulating the PI3K/AKT/mTOR pathway [39]. Methylprednisolone treatment ameliorated hepatocyte apoptosis and autophagy in CoA-induced AIH through the activated AKT/mTOR signalling pathway [40]. In line with these results, we found that itaconate upregulated the levels of p-AKT/AKT and p-mTOR/mTOR to inhibit autophagy *in vivo*. As a consequence, activated mTOR inhibited autophagy and reduced the number of autolysosomes, preventing autophagic cell death [41]. mTOR pathway-sensing environmental cues modulate DC differentiation and immune functions, but the regulation mechanism of itaconate on DCs by the mTOR pathway is not well-understood. Activation of mTOR reduces endogenous antigen presentation on MHC-II molecules by blocking DC autophagy, which limits T cell activation [31]. Inhibition of mTOR with rapamycin augments the production of proinflammatory cytokines; in contrast, activation of mTOR by deletion of TSC2 alleviates proinflammatory cytokine release [42]. We validated *in vivo* that itaconate is a pivotal negative determinant of DC function that regulates autophagy via the mTOR signalling pathway in AIH. mTOR-deleted DCs augmented chronic liver injury and exacerbated IL-6 production by promoting autophagy. MHY1485 alleviated liver inflammation and proinflammation cytokine production by blocking autophagy. Itaconate may affect DCs via the following mechanism: mTOR signalling in DCs functions as a brake to restrain excessive autoimmunity by blocking autophagy, maintaining proper immune homeostasis by inhibiting DC maturation and promoting Treg cells proliferation (data not shown). However, the impact of Itaconate on the mTOR signalling may be indirect, other mechanisms may be involved and further research is required to clarify the molecular mechanism.

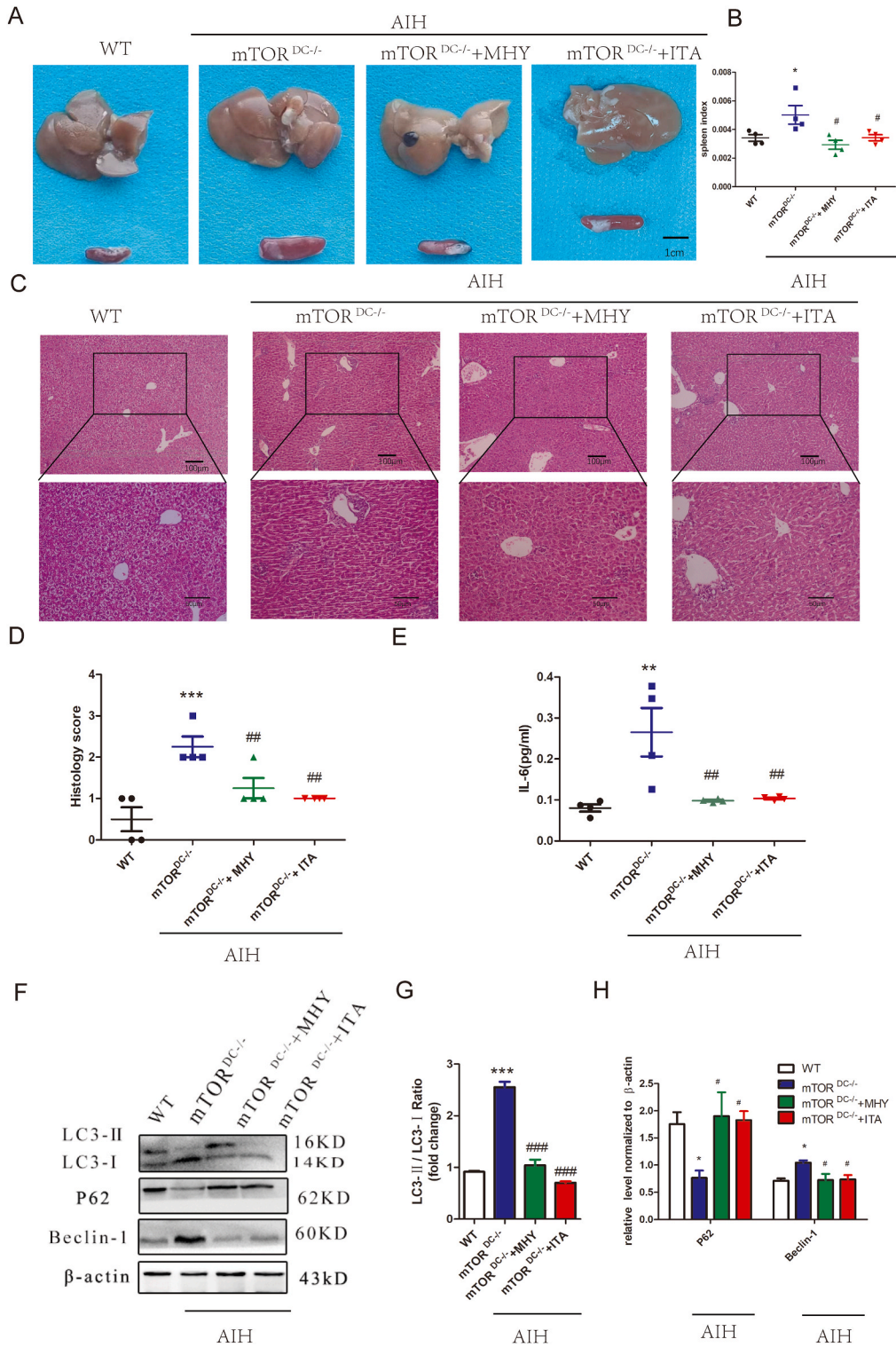


Fig. 7. Itaconate alleviated S100-induced liver inflammation and autophagy in mTOR^{DC-/-} AIH mice. mTOR^{DC-/-} mice were injected intravenously with S100 protein subcomponent combined with Freund's adjuvant. MHY1485(10 mg/kg, 2 days) or itaconate were injected tail intravenously on days 21,23.(A)Liver and spleen tissues were isolated and photographed (scale bar = 1 cm). (B) the spleen index (n = 4 per group). (C,D) Representative micrographs of Haematoxylin and eosin staining with semiquantitative analysis of liver inflammation in indicated groups; scale bar = 50 μm. (E) Serum concentrations of IL-6 were detected via ELISA. (F) Western blot for LC3, p62 and beclin-1 in the liver tissues; β-actin was used as the internal control. (G)(H) Quantitative analysis of the protein levels of the LC3-II/LC3-I ratio and p62 and beclin-1. Values represent

the mean \pm S. D at each time point. Data are shown as the mean \pm SEM of three independent experiment. * $P < 0.05$, ** $P < 0.01$ and *** $P < 0.001$ vs WT. # $P < 0.05$, ## $P < 0.01$ and ### $P < 0.001$ vs mTOR^{DC-/-} mice. WT, wild type; mTOR^{DC-/-}, the conditional knockout mouse bearing floxed mTOR with a CD11c-Cre deletion strain. MHY1485 (an agonist of mTOR); KD, kilodalton.

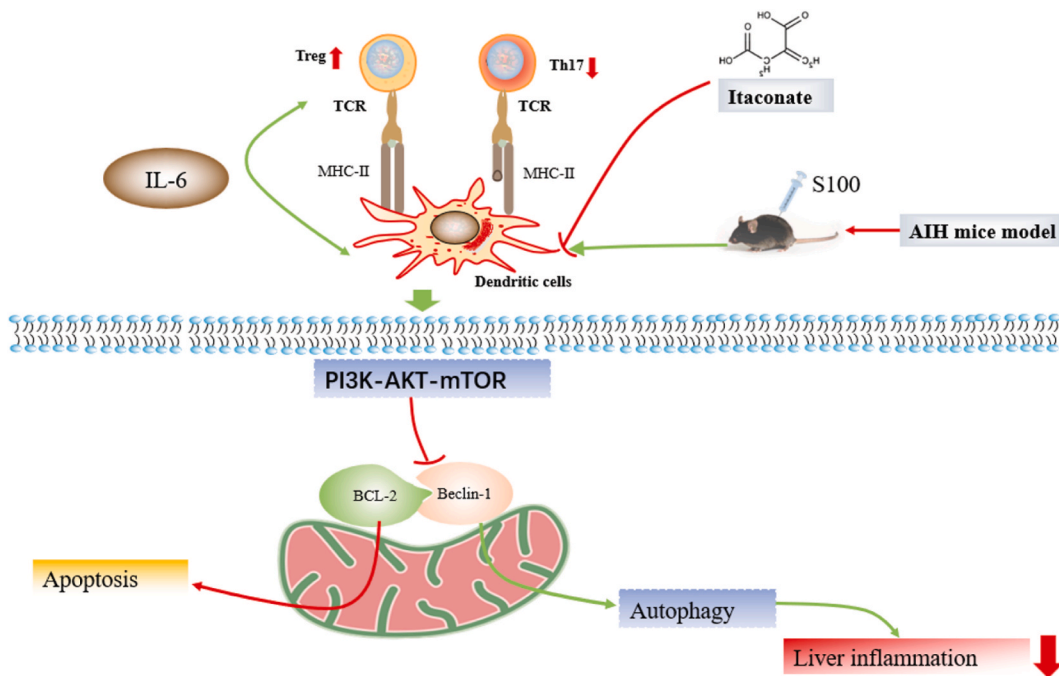


Fig. 8. The graphical abstract. Itaconate exert anti-inflammatory activity via PI3K/AKT/mTOR pathway-mediated inhibition of dendritic cell maturation and autophagy in S100 induced AIH. Itaconate treatment suppressed the maturation of DCs, reprogrammed the reciprocal differentiation of Th17 and Tregs, activated PI3K/Akt/mTOR signaling, ameliorated mitochondria-mediated autophagy dysfunction, and attenuated liver inflammation in AIH.

5. Conclusions

In summary, our study identified the roles of itaconate in the immune function of DCs and the mechanisms of itaconate in AIH, suggesting that itaconate induced DC immune tolerance by decreasing glycolysis and regulating the balance of Th17 and Tregs to prevent AIH. Itaconate treatment ameliorated mitochondria-mediated autophagy dysfunction via the PI3K/AKT/mTOR pathway in AIH (Fig. 8), which may provided a strategy for AIH treatment. Although, S100 induced liver injury could effectively mimics liver injury in human AIH, the mechanisms involved in immune-induced liver injury are complex, and further research is required to elucidate the exact mechanism. The study was performed using mice and cellular experiments, therefor studied on the anti-inflammatory effects of itaconate on human AIH are needed in the future for verification.

Author contribution statement

Qiyu Zhang: Conceived and designed the experiments; Performed the experiments; Analysed and interpreted the data; Wrote the paper.

Haixia Zhao and Qiuxia Zheng: Performed the experiments.

Yang Luo and Xiaofeng Wei: Contributed reagents, materials, analysis tools or data.

Xun Li: Conceived and designed the experiments.

Data availability statement

Data will be made available on general purpose repositories (Mendeley Data, V1, <https://doi.org/10.17632/p5t4pfmncn.1>).

Funding statement

Prof. Xun Li was supported by Grants from the National Natural Science Foundation of China (82060119). Dr. Qiyu Zhang was supported by the Grants from Hospital Fund of The First Hospital of Lanzhou University (ldyyyn2018-45) and Health Industry

Scientific Research Project (GSWSKY- 2018-23).

Declaration of competing interest

The authors declare that they have no known competing financial interests or personal relationships that could have appeared to influence the work reported in this paper.

Acknowledgments

We thank the members of the B.R.M and I.P. labs for their technical assistance and gene knockout mice and thank all the reviewers who participated in the review and Editage (www.editage.cn) for English language editing.

Appendix A. Supplementary data

Supplementary data to this article can be found online at <https://doi.org/10.1016/j.heliyon.2023.e17551>.

References

- [1] D. Vergani, B. Terziroli Beretta-Piccoli, G. Mieli-Vergani, A reasoned approach to the treatment of autoimmune hepatitis, *Dig. Liver Dis.* 53 (11) (2021) 1381–1393, <https://doi.org/10.1016/j.dld.2021.05.033>.
- [2] Y.H. Oo, S.G. Hubscher, D.H. Adams, Autoimmune hepatitis: new paradigms in the pathogenesis, diagnosis, and management, *Hepatol. Int.* 4 (2) (2010) 475–493, [10.1007/s12072-010-9183-5](https://doi.org/10.1007/s12072-010-9183-5).
- [3] G. Mieli-Vergani, D. Vergani, A.J. Czaja, M.P. Manns, E.L. Krawitt, J.M. Vierling, A.W. Lohse, A.J. Montano-Loza, Autoimmune hepatitis, *Nat. Rev. Dis. Prim.* 4 (2018), 18017, <https://doi.org/10.1038/nrdp.2018.17>, 2018.
- [4] Z. Zaslona, L.A.J. O'Neill, Cytokine-like roles for metabolites in immunity, *Mol. Cell.* 78 (5) (2020) 814–823, <https://doi.org/10.1016/j.molcel.2020.04.002>.
- [5] F. Basit, T. Mathan, D. Sancho, I.J.M. de Vries, Human dendritic cell subsets undergo distinct metabolic reprogramming for immune response, *Front. Immunol.* 9 (2018) 2489, <https://doi.org/10.3389/fimmu.2018.02489>.
- [6] A.C. Trombetta, S. Soldano, P. Contini, V. Tomatis, B. Ruaro, S. Paolino, R. Brizzolara, P. Montagna, A. Sulli, C. Pizzorni, V. Smith, M. Cutolo, A circulating cell population showing both M1 and M2 monocyte/macrophage surface markers characterizes systemic sclerosis patients with lung involvement, *Respir. Res.* 19 (2018) 186, [10.1186/s12931-018-0891-z](https://doi.org/10.1186/s12931-018-0891-z).
- [7] Q. Wang, X.L. Li, Y. Mei, J.C. Ye, W. Fan, G.H. Cheng, M.S. Zeng, G.K. Feng, The anti-inflammatory drug dimethyl Itaconate protects against colitis-associated colorectal cancer, *J. Mol. Med. (Berl.)* 98 (10) (2020) 1457–1466, <https://doi.org/10.1007/s00109-020-01963-2>.
- [8] Z. Yi, M. Deng, M.J. Scott, G. Fu, P.A. Loughran, Z. Lei, S. Li, P. Sun, C. Yang, W. Li, H. Xu, F. Huang, T.R. Billiar, Immune-responsive gene 1/itaconate activates nuclear factor erythroid 2-related factor 2 in hepatocytes to protect against liver ischemia-reperfusion injury, *Hepatology* 72 (4) (2020) 1394–1411, [10.1002/2fhep.31147](https://doi.org/10.1002/2fhep.31147).
- [9] C. Tang, X. Wang, Y. Xie, X. Cai, N. Yu, Y. Hu, Z. Zheng, 4-Octyl itaconate activates Nrf2 signaling to inhibit pro-inflammatory cytokine production in peripheral blood mononuclear cells of systemic lupus erythematosus patients, *Cell. Physiol. Biochem.* 51 (2) (2018) 979–990, <https://doi.org/10.1159/000495400>.
- [10] B. Ruaro, S. Soldano, V. Smith, S. Paolino, P. Contini, P. Montagna, C. Pizzorni, A. Casabella, S. Tardito, A. Sulli, M. Cutolo, Correlation between circulating fibrocytes and dermal thickness in limited cutaneous systemic sclerosis patients: a pilot study, *Rheumatol. Int.* 39 (8) (2019) 1369–1376, <https://doi.org/10.1007/s00296-019-04315-7>.
- [11] J. Henderson, L. Duffy, R. Stratton, D. Ford, S. O'Reilly, Metabolic reprogramming of glycolysis and glutamine metabolism are key events in myofibroblast transition in systemic sclerosis pathogenesis, *J. Cell Mol. Med.* 24 (23) (2020) 14026–14038, <https://doi.org/10.1111/jcmm.16013>.
- [12] T. Cordes, M. Wallace, A. Michelucci, A.S. Divakaruni, S.C. Sapcararu, C. Sousa, H. Koseki, P. Cabrales, A.N. Murphy, K. Hiller, C.M. Metallo, Immuno-responsive gene 1 and itaconate inhibit succinate dehydrogenase to modulate intracellular succinate Levels, *J. Biol. Chem.* 291 (27) (2016) 14274–14284, <https://doi.org/10.1074/jbc.m115.685792>.
- [13] V. Lampropoulou, A. Sergushichev, M. Bambouskova, S. Nair, E.E. Vincent, E. Loginicheva, L. Cervantes-Barragan, X. Ma, S.C. Huang, T. Griss, C.J. Weinheimer, S. Khader, G.J. Randolph, E.J. Pearce, R.G. Jones, A. Diwan, M.S. Diamond, M.N. Artyomov, Itaconate links inhibition of succinate dehydrogenase with macrophage metabolic remodeling and regulation of inflammation, *Cell Metabol.* 24 (1) (2016) 158–166, [10.1155%2F2020%2F5404780](https://doi.org/10.1155%2F2020%2F5404780).
- [14] W. Qin, K. Qin, Y. Zhang, W. Jia, Y. Chen, B. Cheng, L. Peng, N. Chen, Y. Liu, W. Zhou, Y.L. Wang, X. Chen, C. Wang, S-glycosylation-based cysteine profiling reveals regulation of glycolysis by Itaconate, *Nat. Chem. Biol.* 15 (10) (2019) 983–991, <https://doi.org/10.1038/s41589-019-0323-5>.
- [15] S.T. Liao, C. Han, D.Q. Xu, X.W. Fu, J.S. Wang, L.Y. Kong, 4-Octyl Itaconate inhibits aerobic glycolysis by targeting GAPDH to exert anti-inflammatory effects, *Nat. Commun.* 10 (1) (2019) 5091, <https://doi.org/10.1038/s41467-019-13078-5>.
- [16] R.L. Wu, F. Chen, N. Wang, D. Tang, R. Kang, ACOD1 in immunometabolism and disease, *Cell. Mol. Immunol.* 17 (8) (2020) 822–833, <https://doi.org/10.1038/s41423-020-0489-5>.
- [17] A.K. Jaiswal, J. Yadav, S. Makhija, S. Mazumder, A.K. Mitra, A. Suryawanshi, M. Sandey, A. Mishra, Irg1/Itaconate metabolic pathway is a crucial determinant of dendritic cells immune-priming function and contributes to resolute allergen-induced airway inflammation, *Mucosal Immunol.* 15 (2) (2022) 301–313, <https://doi.org/10.1038/s41385-021-00462-y>.
- [18] R.G. Knodell, K.G. Ishak, W.C. Black, T.S. Chen, R. Craig, N. Kaplowitz, T.W. Kiernan, J. Wollman, Formulation and application of numerical scoring system for dendritic cell immunological activity in asymptomatic chronic active hepatitis, *Hepatology* 1 (5) (1981) 431–435, <https://doi.org/10.1002/hep.1840010511>.
- [19] E.D. Hu, D.Z. Chen, J.L. Wu, F.B. Lu, L. Chen, M.H. Zheng, H. Li, Y. Huang, J. Li, X.Y. Jin, Y.W. Gong, Z. Lin, X.D. Wang, L.M. Xu, Y.P. Chen, High fiber dietary and sodium butyrate attenuate experimental autoimmune hepatitis through regulation of immune regulatory cells and intestinal barrier, *Cell. Immunol.* 328 (2018) 24–32, <https://doi.org/10.1016/j.cellimm.2018.03.003>.
- [20] S.J. Kim, B. Diamond, Modulation of tolerogenic dendritic cells and autoimmunity, *Semin. Cell Dev. Biol.* 41 (2015) 49–58, <https://doi.org/10.1016/j.semcdb.2014.04.020>.
- [21] L.A.J. O'Neill, E.J. Pearce, Immunometabolism governs dendritic cell and macrophage function, *J. Exp. Med.* 213 (1) (2016) 15–23, <https://doi.org/10.1084/jem.20151570>.
- [22] A. Waisman, D. Lukas, B.E. Clausen, N. Yagci, Dendritic cells as gatekeepers of tolerance, *Semin. Immunopathol.* 39 (2) (2017) 153–163, <https://doi.org/10.1007/s00281-016-0583-z>.
- [23] N. Sukhbaatar, M. Hengstschlager, T. Weichhart, mTOR-mediated regulation of dendritic cell differentiation and function, *Trends Immunol.* 37 (11) (2016) 778–789, <https://doi.org/10.1016/j.it.2016.08.009>.

- [24] S. Singh, P.K. Singh, A. Jha, P. Naik, J. Joseph, S. Giri, A. Kumar, Integrative metabolomics and transcriptomics identifies Itaconate as an adjunct therapy to treat ocular bacterial infection, *Cell Rep. Med.* 2 (5) (2021), 100277, <https://doi.org/10.1016/j.xcrm.2021.100277>.
- [25] S. Sozzani, A. Del Prete, D. Bosisio, Dendritic cell recruitment and activation in autoimmunity, *J. Autoimmun.* 85 (2017) 126–140, <https://doi.org/10.1016/j.jaut.2017.07.012>.
- [26] C. Tomiyama, H. Watanabe, Y. Izutsu, M. Watanabe, T. Abo, Suppressive role of hepatic dendritic cells in concanavalin A-induced hepatitis, *Clin. Exp. Immunol.* 166 (2) (2011) 258–268, <https://doi.org/10.1111/j.1365-2249.2011.04458.x>.
- [27] Z. He, X. Zhu, Z. Shi, T. Wu, L. Wu, Metabolic regulation of dendritic cell differentiation, *Front. Immunol.* 10 (2019) 410.
- [28] J. Liu, X. Cao, Regulatory dendritic cells in autoimmunity: a comprehensive review, *J. Autoimmun.* 63 (2015) 1–12, <https://doi.org/10.1016/j.jaut.2015.07.011>.
- [29] C.C. Gross, H. Jonuleit, H. Wiendl, Fulfilling the dream: tolerogenic dendritic cells to treat multiple sclerosis, *Eur. J. Immunol.* 42 (3) (2012) 569–572, <https://doi.org/10.1002/eji.201242402>.
- [30] B. Everts, E. Amiel, S.C. Huang, A.M. Smith, C.H. Chang, W.Y. Lam, V. Redmann, T.C. Freitas, J. Blagih, G.J. van der Windt, M.N. Artyomov, R.G. Jones, E. L. Pearce, E.J. Pearce, TLR-driven early glycolytic reprogramming via the kinases TBK1-IKK ϵ supports the anabolic demands of dendritic cell activation, *Nat. Immunol.* 15 (4) (2014) 323–332, <https://doi.org/10.1038/ni.2833>.
- [31] K. Mahnke, T.S. Johnson, S. Ring, A.H. Enk, Tolerogenic dendritic cells and regulatory T cells: a two-way relationship, *J. Dermatol. Sci.* 46 (3) (2007) 159–167, <https://doi.org/10.1016/j.jdermsci.2007.03.002>.
- [32] S. Wan, C. Xia, L. Morel, IL-6 produced by dendritic cells from lupus-prone mice inhibits CD4+CD25+ T cell regulatory functions, *J. Immunol.* 178 (1) (2007) 271–279, <https://doi.org/10.4049/jimmunol.178.1.271>.
- [33] P. Ravanan, I.F. Srikumar, P. Talwar, Autophagy: the spotlight for cellular stress responses, *Life Sci.* 188 (2017) 53–67, <https://doi.org/10.1016/j.lfs.2017.08.029>.
- [34] T. Szekerczes, A. Gogl, I. Illyes, J. Mandl, K. Borka, A. Kiss, Z. Schaff, G. Lendvai, K. Werling, Autophagy, mitophagy and MicroRNA expression in chronic hepatitis C and autoimmune hepatitis, *Pathol. Oncol. Res.* 26 (4) (2020) 2143–2151, <https://doi.org/10.1007/s12253-020-00799-y>.
- [35] X. Fan, R. Men, C. Huang, M. Shen, T. Wang, Y. Ghnewa, Y. Ma, T. Ye, L. Yang, Critical roles of conventional dendritic cells in autoimmune hepatitis via autophagy regulation, *Cell Death Dis.* 11 (1) (2020) 23.
- [36] S. Sridhar, Y. Botbol, F. Macian, A.M. Cuervo, Autophagy and disease: always two sides to a problem, *J. Pathol.* 226 (2) (2012) 255–273, <https://doi.org/10.1002/path.3025>.
- [37] S.K. Wculek, S.C. Khouili, E. Priego, I. Heras-Murillo, D. Sancho, Metabolic control of dendritic cell functions: digesting information, *Front. Immunol.* 10 (2019) 775.
- [38] J.H. Han, H.S. Park, D.H. Lee, J.H. Jo, K.S. Heo, C.S. Myung, Regulation of autophagy by controlling Erk1/2 and mTOR for platelet-derived growth factor-BB-mediated vascular smooth muscle cell phenotype shift, *Life Sci.* 267 (2021), 118978, <https://doi.org/10.1016/j.lfs.2020.118978>.
- [39] S. Xu, L. Wu, Q. Zhang, J. Feng, S. Li, J. Li, T. Liu, W. Mo, W. Wang, X. Lu, Q. Yu, K. Chen, Y. Xia, J. Lu, L. Xu, Y. Zhou, X. Fan, C. Guo, Pretreatment with propylene glycol alginate sodium sulfate ameliorated concanavalin A-induced liver injury by regulating the PI3K/Akt pathway in mice, *Life Sci.* 185 (2017) 103–113, <https://doi.org/10.1016/j.lfs.2017.07.033>.
- [40] X. Fan, R. Men, H. Wang, M. Shen, T. Wang, T. Ye, X. Luo, L. Yang, Methylprednisolone decreases mitochondria-mediated apoptosis and autophagy dysfunction in hepatocytes of experimental autoimmune hepatitis model via the akt/mTOR signaling, *Front. Pharmacol.* 10 (2019) 1189.
- [41] L. Yu, L. Strandberg, M.J. Lenardo, The selectivity of autophagy and its role in cell death and survival, *Autophagy* 4 (5) (2008) 567–573, <https://doi.org/10.4161/auto.5902>.
- [42] T. Weichhart, G. Costantino, M. Poglitsch, M. Rosner, M. Zeyda, K.M. Stuhlmeier, T. Kolbe, T.M. Stulnig, W.H. Horl, M. Hengstschlager, M. Muller, M. D. Saemann, The TSC-mTOR signaling pathway regulates the innate inflammatory response, *Immunity* 29 (4) (2008) 565–577, <https://doi.org/10.1016/j.immuni.2008.08.012>.